



Cent. Eur. J. Energ. Mater. 2018, 15(3): 405-419; DOI: 10.22211/cejem/94788
Research paper

Synthesis, Characterization and Thermal Decomposition of a New Energetic Salt of 1*H*,1'*H*-5,5'-Bistetrazole-1,1'-diol

**Lipengcheng Xiao¹, Bo Jin^{1*}, Yu Shang¹, Qiangqiang Liu¹,
Zhicheng Guo², Rufang Peng¹**

¹ *State Key Laboratory Cultivation Base for Nonmetal Composites and Functional Materials, Southwest University of Science and Technology, Mianyang 621010, China*

² *School of Nation Defence Science and Technology, Southwest University of Science and Technology, Mianyang 621010, China*

**E-mail: jinbo0428@163.com*

Abstract: 1,1-Dimethylbiguanidium 1*H*,1'*H*-5,5'-bistetrazole-1,1'-diolate (MGBTO), a novel nitrogen-rich energetic salt, was synthesized by cation exchange. Its structure was characterized by elemental analysis, FTIR, NMR, DTA and TG-DTG. Single crystal X-ray diffraction analysis revealed that MGBTO was crystallized in the monoclinic space group C2/c. Thermal analysis demonstrated that its thermal stability extended up to 531.1 K. The nonisothermal kinetic and apparent thermodynamic parameters of the exothermic decomposition of MGBTO were determined by the Kissinger and Ozawa methods. Its detonation velocity and detonation pressure were calculated on the basis of the Kamlet-Jacobs equation and were 6342 m·s⁻¹ and 15.78 GPa, respectively. The impact and friction sensitivities of MGBTO were quantified using standard BAM (10 kg drop hammer) procedures. The results revealed that the salt has good mechanical sensitivity (FS > 120 N, IS > 40 J), thus indicating its potential applications as an energetic material.

Keywords: 1,1-dimethylbiguanidium 1*H*,1'*H*-5,5'-bistetrazole-1,1'-diolate (MGBTO), single crystal, thermal properties, energetic properties

1 Introduction

A unique class of highly energetic materials based on nitrogen-rich heterocyclic ionic salts has been developed over recent decades, due to the observation that the detonation performance of heterocyclic ionic salts can be easily modified with different combinations of anions and cations [1-7]. The tetrazole ring and its derivatives have attracted extensive interest because of their unique and excellent properties, such as high nitrogen content, high formation enthalpy, and good stability [8]. Among all of the strategies used to improve the detonation performance of energetic materials, the use of N-oxides is a special approach that facilitates the achievement of oxygen balance [8-15]. Fischer and his coworkers synthesized a series of 1*H*,1'*H*-5,5'-bistetrazole-1,1'-diolate (BTO) salts [8, 16] and showed that the excellent performance of dihydroxylammonium 1*H*,1'*H*-5,5'-bistetrazole-1,1'-diolate (TKX-50) is comparable with that of CL-20. Since then, researchers have begun to pay attention to BTO-based energetic salts due to their impact-insensitivity and high-energy [17-22]. Therefore, related research on BTO-based energetic materials should be continued in order to develop potential energetic materials.

In this paper, we report a new energetic compound, 1,1-dimethylbiguanidium 1*H*,1'*H*-5,5'-bistetrazole-1,1'-diolate (MGBTO), which was synthesized by reacting BTO with 1,1-dimethylbiguanidium hydrochloride (metformin hydrochloride). The crystal structure, thermal stability, nonisothermal kinetics analysis, sensitivity, calculated molar enthalpy of formation, and calculated detonation properties of MGBTO were investigated, and the results showed that MGBTO has potential applications as a nitrogen-enriched energetic material with good thermal stability and low sensitivity.

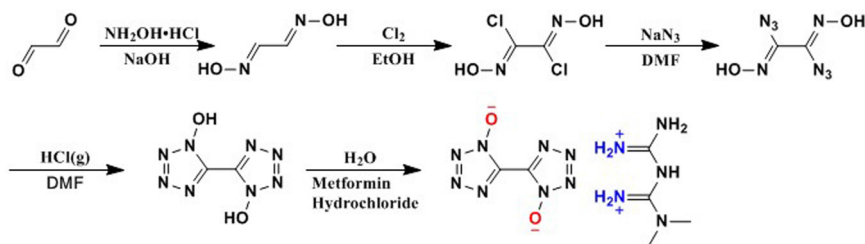
2 Experimental

2.1 Materials and methods

All chemicals were commercially available and used without further purification. FTIR spectra were recorded on a Nicolet-5700 FTIR spectrometer using pressed KBr pellets in the wavelength range 400 cm^{-1} to 4000 cm^{-1} . The ^1H and ^{13}C NMR spectra were recorded on a JEOL GSX 600 MHz nuclear magnetic resonance (NMR) spectrometer at 600 MHz and 100 MHz, respectively. Single-crystal diffraction analysis was collected by a Bruker Smart APEX II CCD diffractometer. The thermogravimetric analysis (TG) was performed on a STA6000 instrument, and the temperature was increased from room temperature to above 800 K at a heating rate of 10 $\text{K}\cdot\text{min}^{-1}$ in flowing high-purity nitrogen.

2.2 Synthesis

Dimethylbiganidium 1*H*,1'*H*-5,5'-bistetrazole-1,1'-diolate (MGBTO) was synthesized through cation exchange (Scheme 1). Initially, 1*H*,1'*H*-5,5'-bistetrazole-1,1'-diol dihydrate (H₂BTO·2H₂O) was synthesized in four steps according to a previously reported procedure [8]. Then a mixture of H₂BTO·2H₂O (1 mmol) and 1,1-dimethylbiganidium hydrochloride (1 mmol) in H₂O (5 mL) was heated to reflux for 0.5 h. The white MGBTO salt was recovered by vacuum drying. Finally, a suitable crystal of MGBTO was obtained by slow evaporation of water at room temperature. ¹H NMR (600 MHz, D₂O, 25 °C) δ/ppm: 3.19. ¹³C NMR (100 MHz, [D₆]DMSO, 25 °C) δ/ppm: 135.11, 155.04, 156.15. IR (KBr), ν/(cm⁻¹): 3392(m), 3187(w), 1689(s), 1627(m), 1571(m), 1487(w), 1409(w), 1295(w), 1217(w), 1131(w), 994(w), 841(w), 763(w). Elemental analysis (EA): Found/%: C 22.62, H 4.79, N 57.41; Calculated/%: C 22.71, H 4.76, N 57.38.



Scheme 1. The synthesis of MGBTO

3 Results and Discussion

3.1 Characterization

The structure of MGBTO was characterized by FTIR, ¹H NMR, ¹³C NMR, EA, and single crystal X-ray diffraction. As shown in Figure 1, the IR spectrum of MGBTO shows a sharp, strong band at 1689 cm⁻¹. This band is attributed to the C=N stretching vibrations in the cation. An intense broad band centered at 3392 cm⁻¹ corresponds to the stretching vibrations of N–H. Moreover, absorption bands between 1571 cm⁻¹ and 699 cm⁻¹ show the characteristic pattern of ν(NN), ν(NCN), γ(CN), and δ aromatic ring. These signals are in close agreement with those observed for previously reported BTO salts [8].

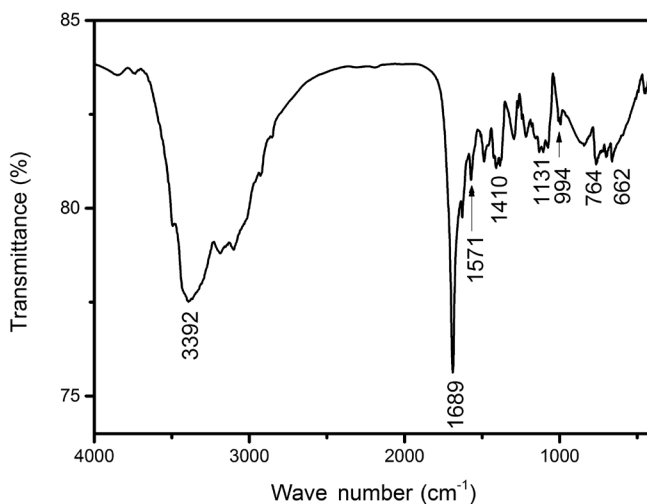


Figure 1. FTIR spectrum of MGBTO

The structure of MGBTO was also confirmed using ^1H and ^{13}C NMR spectra. The ^1H NMR spectrum in D_2O exhibited a signal at $\delta = 3.19$ ppm. This signal is assigned to the hydrogen atoms of the methyl groups in the cation. The resonance at 135.11 ppm in ^{13}C NMR corresponds to the carbon atoms in the BTO anion, whereas the remaining signals at 155.05 ppm and 156.15 ppm are assigned to the cation.

Four solution combinations were prepared to obtain a suitable crystal for X-ray crystallography. Only one, however, yielded a suitable single crystal through slow evaporation of water at room temperature. The crystals yielded by the other three solvents all exhibited disordered atoms. Table 1 presents a summary of the crystallographic data and refinement details for MGBTO. The X-ray crystallographic data showed that MGBTO crystallizes with a molecule of water of crystallization in the monoclinic space group $C2/c$, with a calculated density of 1.487 g/cm^3 based on eight molecules packed in the unit-cell volume of $2834.81(14) \text{ \AA}^3$. The molecular unit is shown in Figure 2. The torsion values of N6-N5-C2-C1 and N6-N7-N8-O2 are 178.62° and 180° , respectively, indicating that the molecules are arranged in a nearly planar bicyclic ring system. The distances between any two adjacent atoms in the BTO anion lay between the lengths of formal single and double bonds [8, 21] due to the influence of the conjugation of negative charges throughout the aromatic ring. Selected bond lengths and angles are listed in Table 2. Data on hydrogen bonds in the molecular structure are presented in Table 3. The packing diagram

of MGBTO built up by hydrogen bonds is shown in Figure 3. Hydrogen bonds are represented by dashed lines. Each N-H of the amino groups in the cation acts as a hydrogen bond donor and bonds with an anion *via* N-H...O (1.894 Å to 2.279 Å) or N-H...N (2.06 Å to 2.526 Å). Water molecules play an important role in cell accumulation. Oxygen atoms in the water molecule form hydrogen bonds and act as H-bond acceptors with cations. The hydrogen atoms form hydrogen bonds and act as H-bond donors with anions.

Table 1. Crystallographic data and structural refinement parameters of MGBTO

Formula	C ₆ H ₁₅ N ₁₃ O ₃
Formula weight	317.31
CCDC number	1564682
Crystal size [mm ³]	0.19×0.18×0.17
Crystal system	Monoclinic
Space group	C2/c
a [Å]	18.1044(6)
b [Å]	11.0024(2)
c [Å]	15.8272(4)
α [°]	90
β [°]	115.949(3)
γ [°]	90
V [Å ³]	2834.81(14)
Z	8
ρ _{calcd} [g·cm ⁻³]	1.487
μ [mm ⁻¹]	1.047
T [K]	150.15
F(000)	1327
R _{int.}	0.0215
Data	2456
Restraints	0
Parameters	201
R ₁ ^a (I > 2σ (I))	0.049
ωR ₂ ^b (I > 2σ (I))	0.1286
GOF ^c on F ²	1.057

$$^a R_1 = \frac{\sum ||F_o| - |F_c||}{\sum |F_o|}$$

$$^b \omega R_2 = \frac{[\omega (F_o^2 - F_c^2)^2]}{\omega (F_o^2)^2}^{1/2}$$

^c GOF= Goodness of Fit

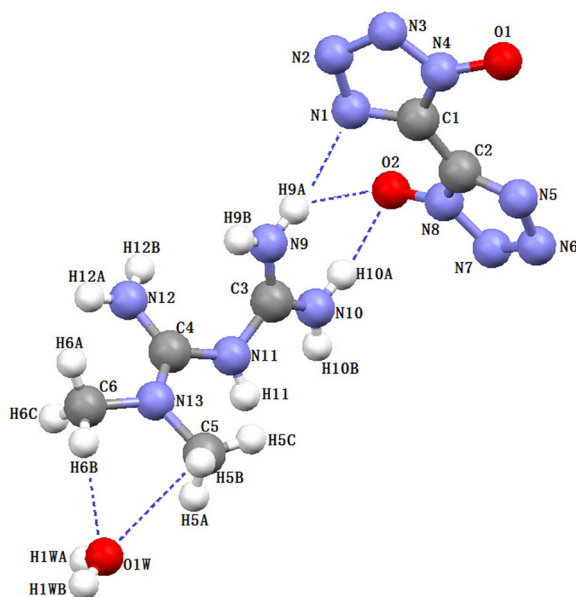


Figure 2. Ball-and-stick molecular structure of MGBTO. Dashed lines indicate hydrogen bonds

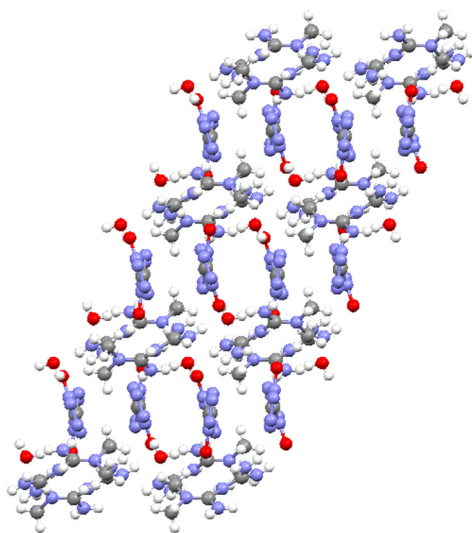


Figure 3. Packing diagram of MGDTO viewed down the b axis

Table 2. Selected bond lengths [\AA] and angles [$^\circ$] of MGBT0

Atom	Atom	Length [\AA]	Atom	Atom	Atom	Angle [$^\circ$]
N9	C3	1.320(2)	C3	N11	C4	125.09(14)
N10	C3	1.313(2)	C4	N13	C5	123.28(15)
N11	C3	1.364(2)	C4	N13	C6	119.57(15)
N11	C4	1.387(2)	C6	N13	C5	116.95(15)
N12	C4	1.315(2)	N9	C3	N11	120.30(16)
N13	C4	1.317(2)	N10	C3	N9	121.45(16)
N13	C5	1.467(2)	N10	C3	N11	118.24(15)
N13	C6	1.463(2)	N12	C4	N11	118.69(15)
O1	N4	1.3317(19)	N12	C4	N13	122.95(16)
O2	N8	1.3246(19)	N13	C4	N11	118.34(15)
N1	N2	1.346(2)	C1	N1	N2	105.66(15)
N1	C1	1.332(2)	N3	N2	N1	111.20(15)
N2	N3	1.316(2)	N2	N3	N4	105.98(14)
N3	N4	1.337(2)	O1	N4	N3	121.21(14)
N4	C1	1.347(2)	O1	N4	C1	129.95(15)
C1	C2	1.447(3)	N3	N4	C1	108.82(14)
			N1	C1	N4	108.32(16)
			N1	C1	C2	125.98(16)
			N4	C1	C2	125.69(16)
			N5	C2	N8	108.29(15)

Table 3. Hydrogen bonds of MGBT0

D-H \cdots A	d(D-H)	d(H \cdots A)	d(D \cdots A)
N9-H9A \cdots O2#1	0.860	2.279	2.973
N9-H9A \cdots N1#1	0.860	2.526	3.220
N9-H9B \cdots N12	0.860	2.522	2.937
N9-H9B \cdots O1	0.860	2.151	2.878
N10-H10A \cdots O2#1	0.860	1.96	2.740
N10-H10B \cdots O1W#2	0.860	2.006	2.844
N11-H11 \cdots O1#3	0.860	2.072	2.891
N12-H12A \cdots N6#4	0.860	2.06	2.864
N12-H12B \cdots O2#5	0.860	1.894	2.740
C5-H5B \cdots O1W#6	0.980	2.616	3.247
C6-H6B \cdots O1W	0.980	2.506	3.439
O1W-H1WA \cdots N2#7	0.860	2.074	2.899
O1W-H1WB \cdots O1#6	0.838	1.936	2.741
O1W-H1WB \cdots N4#6	0.838	2.585	3.335

Symmetry transformations used to generate equivalent atoms: #1 $[-x+1, y, -z+1/2]$;

#2 $[x, -y, z-1/2]$; #3 $[-x+1/2, y-1/2, -z+1/2]$; #4 $[-x+1/2, y+1/2, -z+1/2]$;

#5 $[x-1/2, -y+1/2, z-1/2]$; #6 $[-x+1/2, y-1/2, -z+1]$; #7 $[x-1/2, y-1/2, z]$

3.2 Thermal decomposition behaviour

The thermal stability and decomposition behaviour of MGBTO were investigated through differential thermal analysis (DTA) and thermogravimetry-derivative thermogravimetry (TG-DTG) measurements obtained at a rate of 10 K/min. The DTA curve of the salt (Figure 4) exhibits only one exothermic peak at 531.1 K throughout the entire thermal decomposition, indicating that it has good thermal stability under an air atmosphere. A small endothermic peak at 418.2 K corresponds to the loss of crystal water. The TG-DTG curve (Figure 5) obtained under flowing high-purity nitrogen shows two mass loss stages. The salt undergoes its first mass loss process from 386.6 K to 431.5 K. This process results in a mass loss of 4.9%, which corresponds to the loss of one water molecule. A significant mass loss of 64.7% occurs from 431.5 K onwards and may be attributed to the collapse of the main framework and its transformation into volatile gaseous products.

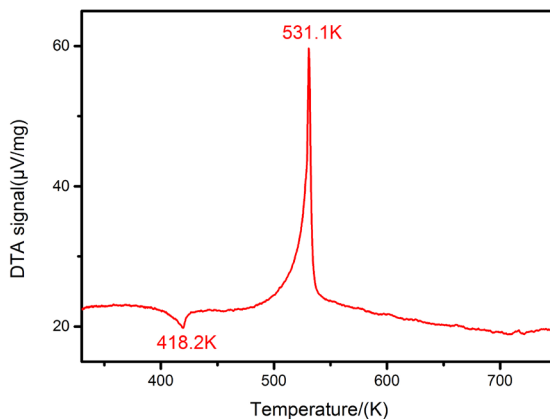


Figure 4. DTA curve of MGBTO

Thermogravimetric analysis tandem infrared spectroscopy was used to identify the volatile gaseous products of MGBTO thermal decomposition. Figure 6 depicts the FTIR spectra of the gaseous MGBTO decomposition products at different temperatures during the whole heating process. Due to the low water content of the salt, the infrared peak of the water is not evident and overlaps with baseline fluctuations. The decomposition products of its second weight loss phase, include NH_3 ($1376\text{--}1470\text{ cm}^{-1}$, $808\text{--}1016\text{ cm}^{-1}$), N_2O ($2194\text{--}2330\text{ cm}^{-1}$, $1188\text{--}1341\text{ cm}^{-1}$), CN group ($\sim 2250\text{ cm}^{-1}$) [23], and C-H compounds ($2783\text{--}3074\text{ cm}^{-1}$) [24], which are derived from the cation and anion. Gases are released along with the collapse of the main framework during

the decomposition of MGBTO. Infrared signals had almost disappeared by the time the temperature had reached 617.2 K, thus proving that the compound has almost completely decomposed. The thermal decomposition investigation shows a possible decomposition mechanism as shown in Figure 7.

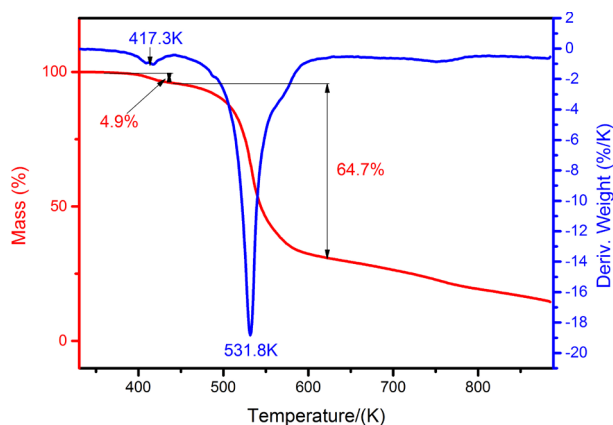


Figure 5. TG-DTG curve of MGBTO

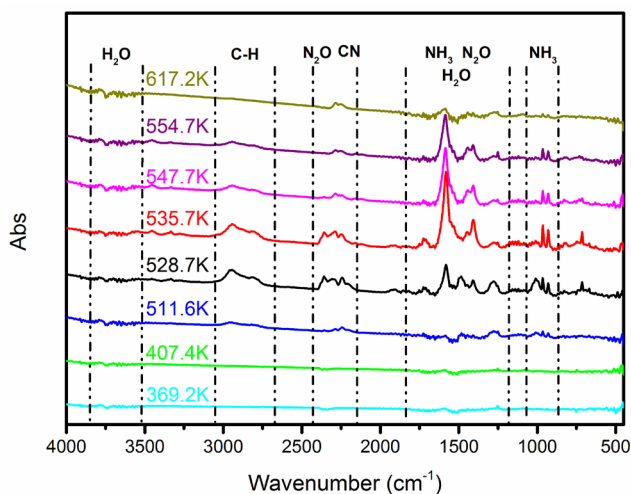


Figure 6. FTIR spectra of the gaseous products from MGBTO during decomposition at individual temperatures

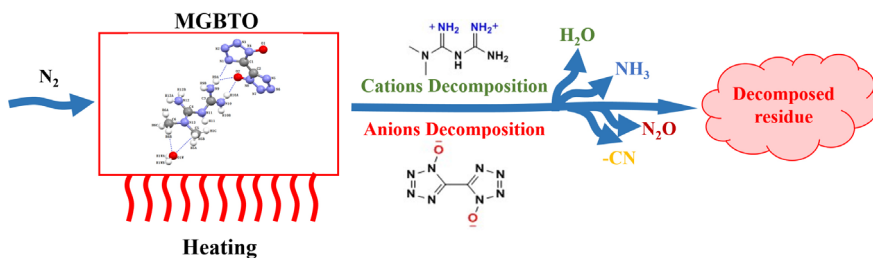


Figure 7. Thermal decomposition mechanism for MGBTO

3.3 Nonisothermal kinetics analysis

The potential of MGBTO as an energetic material was explored through theoretical calculations of its decomposition mechanism, apparent activation energy, and pre-exponential constant. The kinetic parameters were calculated using the Kissinger [25] (Equation 1) and Ozawa [26, 27] (Equation 2) methods:

$$\ln[\beta / T_p^2] = \ln[AR / E_a] - [E_a / RT_p] \quad (1)$$

$$\lg\beta = c - 0.4567E_a / RT_F \quad (2)$$

where E_a is the apparent activation energy (kJ/mol), A is the pre-exponential factor (s^{-1}), R is the gas constant ($J/mol \cdot K$), c is a constant, β is the linear heating rate (K/min), and T_p is the corresponding peak temperature (K).

The peak temperatures of the exothermic process at heating rates of 5 K/min, 10 K/min, 15 K/min, and 20 K/min were 517.3 K, 531.1 K, 537.1 K, and 543.5 K (Figure 8), respectively. The apparent activation energies calculated through the Kissinger and Ozawa methods are listed in Table 4. The Arrhenius equation for MGBTO decomposition can be expressed using the E_a obtained (the average value of the Kissinger method and Ozawa method) and $\ln A$ values, as follows: $\ln k = 18.89 - 118.05 \times 10^3/RT$ for MGBTO. This equation can be used to estimate the rate constant of the thermal decomposition process of the main frame of this salt.

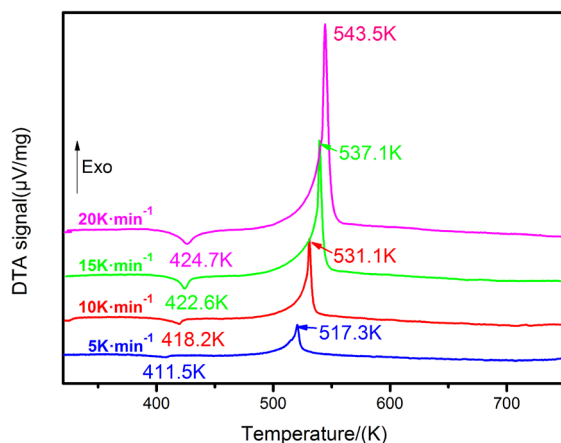


Figure 8. DTA curve of MGBTO at different heating rates

Table 4. Kinetic parameters obtained through the Kissinger and Ozawa methods

β [K·min ⁻¹]	T_p [K]	Kissinger method			Ozawa method	
		E_a [kJ·mol ⁻¹]	$\ln A$	r	E_a [kJ·mol ⁻¹]	r
5	517.3	116.77	18.89	0.9935	119.33	0.9943
10	531.1					
15	537.1					
20	543.5					

3.4 Detonation parameters and sensitivity

Detonation velocity (D) and detonation pressure (P) are important parameters of energetic salts. The detonation parameters were estimated using the empirical Kamlet-Jacobs equations [28] (Equations 3 and 4). Calculating the Q value is critical to obtaining the D and P values. Q is the explosive detonation chemical energy. This value was obtained using the value of the heat of formation (HOF) and molecular formula of MGBTO. Here, the parameters N , M , and Q were calculated according to the chemical composition of each explosive (shown in Table 5) [29].

$$D = 1.01(\overline{NM}^{1/2} Q^{1/2})^{1/2} (1+1.3\rho) \quad (3)$$

$$P = 1.558\rho^2\overline{NM}^{1/2} Q^{1/2} \quad (4)$$

Table 5. Methods for calculating the N , \bar{M} and Q parameters of a $C_aH_bO_cN_d$ explosive

Parameter	Stoichiometric ratio		
	$c \geq 2a + b/2$	$2a + b/2 > c \geq b/2$	$b/2 > c$
N	$(b + 2c + 2d)/4M$	$(b + 2c + 2d)/4M$	$(b + d)/2M$
\bar{M}	$4M/(b + 2c + 2d)$	$(56d + 88c - 8b)/(b + 2c + 2d)$	$(2b + 28d + 32c)/(b + d)$
Q	$(28.9b + 94.05a + 0.239\Delta H_f^0)/M$	$[28.9b + 94.05(c/2 - b/4) + 0.239\Delta H_f^0]/M$	$(57.8c + 0.239\Delta H_f^0)/M$

An accurate prediction of HOF is crucial given that it is used as an index of the “energy content” of energetic compounds. When a salt is evaporated to gas, free acid and base can be generated [30]. According to the literature [30], the standard heat of formation of a salt could be simplified using formulas (5)–(7). The HOF of BTO-based ionic salts can be predicted by the known HOF of the salt with different cations. The HOF of the salt ($L \cdot HA$) is related to the HOF of the constituent base (L) and acid (HA), and $\Delta_r H^0$ is the enthalpy of reaction. The HOF of MGBTO is 201 kJ/mol, according to the HOF of diguanidinium 5,5'-bistetrazole-1,1'-diolate [8, 30]. Taking into account the molecule of crystal water (−109 kJ/mol), the HOF of MGBTO can be 92 kJ/mol.

$$\Delta_r H^0 (L \cdot HA) = \Delta_r H^0 (L) + \Delta_r H^0 (HA) + \Delta_r H^0 \quad (5)$$

$$\Delta_r H^0 (L \cdot HA) - \Delta_r H^0 (L \cdot HB) = \Delta_r H^0 (HA) - \Delta_r H^0 (HB) = Const \quad (6)$$

$$\Delta_r H^0 (L \cdot HA) = \Delta_r H^0 (L \cdot HB) + Const \quad (7)$$

Table 6. Calculation of the parameters of the Kamlet-Jacobs equation

M [$g \cdot mol^{-3}$]	P [$g \cdot cm^{-3}$]	N [$mol \cdot g^{-1}$]	\bar{M} [$g \cdot mol^{-1}$]	ΔH_f [$kJ \cdot mol^{-1}$]
317.31	1.487	0.0441	17.5	92

The value of Q is $617.6 J \cdot g^{-1}$. The detonation velocity and detonation pressure based on the traditional Kamlet-Jacobs equations are $6342 m \cdot s^{-1}$ and $15.78 GPa$, respectively. These values indicate that the detonation performance of MGBTO is close to that of TNT ($6881 m \cdot s^{-1}$, $19.50 GPa$) [31].

Sensitivity deserves significant attention from researchers because it is closely linked with the safety of handling and application of explosives. For safety testing, the sensitivity of MGBTO to impact (IS) and friction (FS) were measured using standard BAM procedures. The results showed that this salt has satisfactory friction sensitivity ($>120 N$) and impact sensitivity ($>40 J$). The 5s detonation point of an explosive is a parameter that indicates

the thermal stability of the material and its ability to be initiated. According to GJB772A-1997, the test results for MGBTO show that it can be initiated and the 5s detonation point (T_{5S}) is 542 K. Therefore, this energetic salt has potential applications as a mechanically insensitive energetic material.

4 Conclusions

A new BTO-based energetic salt was synthesized and its structure was confirmed by single crystal X-ray diffraction and other spectroscopic analyses. Moreover, the detonation properties ($6342 \text{ m}\cdot\text{s}^{-1}$, 15.78 GPa), calculated using the Kamlet-Jacobs equations and molecular stability ($FS > 120 \text{ N}$, $IS > 40 \text{ J}$, $T_d = 531.1 \text{ K}$, $T_{5S} = 542 \text{ K}$) obtained experimentally, indicate that the salt exhibits a proper balance.

Acknowledgements

This work was supported by the Science Challenge Project (Project No. TZ2018004), the National Natural Science Foundation of China (Project No. 21875192, 11602240), the Institute of Chemical Materials, China Academy of Engineering Physics (Project No. 18zh0079) and Open Project of State Key Laboratory Cultivation Base for Nonmetal Composites and Functional (Project No. 14tdfk05).

References

- [1] Liu, Q.; Jin, B.; Peng, R.; Guo, Z.; Zhao, J.; Zhang, Q.; Yu, S. Synthesis, Characterization and Properties of Nitrogen-rich Compounds Based on Cyanuric Acid: a Promising Design in the Development of New Energetic Materials. *J. Mater. Chem. A* **2016**, 4(13): 4971-4981.
- [2] Gao, H.; Shreeve, J. M. Azole-based Energetic Salts. *Chem. Rev.* **2011**, 111(11): 7377-7436.
- [3] Joo, Y. H.; Shreeve, J. M. Nitroimino-tetrazolates and Oxy-nitroimino-tetrazolates. *J. Am. Chem. Soc.* **2010**, 132(42): 15081-15090.
- [4] Joo, Y. H.; Shreeve, J. M. High-density Energetic Mono- or Bis(oxy)-5-Nitroiminotetrazoles. *Angew. Chem. Int. Ed.* **2010**, 49(40): 7320-7323.
- [5] Vo, T. T.; Shreeve, J. M. 1,1-Diamino-2,2-dinitroethene (FOX-7) and 1-Amino-1-hydrazino-2,2-dinitroethene (HFOX) as Amphotères: Bases with Strong Acids. *J. Mater. Chem. A* **2015**, 3(16): 8756-8763.
- [6] Shang, Y.; Jin, B.; Peng, R.; Liu, Q.; Tan, B.; Guo, Z.; Zhao, J.; Zhang, Q. Synthesis

- and Superior Explosive Performance of a Pb(II) Compound with 5,5'-Bistetrazole-1,1'-diolate. *Dalton Trans.* **2016**, 45: 13881-13887.
- [7] Zhang, Q.; Shreeve, J. M. Energetic Ionic Liquids as Explosives and Propellant Fuels: a New Journey of Ionic Liquid Chemistry. *Chem. Rev.* **2014**, 114(20): 10527-10574.
- [8] Fischer, N.; Klapötke, T. M.; Reymann, M.; Stierstorfer, J. Nitrogen-rich Salts of 1H,1'H-5,5'-Bitetrazole 1,1'-Diol: Energetic Materials with High Thermal Stability. *Eur. J. Inorg. Chem.* **2013**, 2013(12): 2167-2180.
- [9] Hafner, K.; Klapötke, T. M.; Schmid, P. C.; Stierstorfer, J. Synthesis and Characterization of Asymmetric 1,2-Dihydroxy-5,5'-Bitetrazole and Selected Nitrogen-rich Derivatives. *Eur. J. Inorg. Chem.* **2015**, 2015(17): 2794-2803.
- [10] Dippold, A. A.; Klapötke, T. M.; Winter, N. Insensitive Nitrogen-rich Energetic Compounds Based on the 5,5'-Dinitro-3,3'-bi-1,2,4-triazol-2-ide Anion. *Eur. J. Inorg. Chem.* **2012**, 2012(21): 3474-3484.
- [11] Yu, Q.; Wang, Z.; Wu, B.; Yang, H.; Ju, X.; Lu, C.; Cheng, G. A Study of N-trinitroethyl-substituted Aminofurazans: High Detonation Performance Energetic Compounds with Good Oxygen Balance. *J. Mater. Chem. A* **2015**, 3(15): 8156-8164.
- [12] Göbel, M.; Karaghiosoff, K.; Klapötke, T. M.; Piercey, D. G.; Stierstorfer, J. Nitrotetrazolate-2N-oxides and the Strategy of N-oxide Introduction. *J. Am. Chem. Soc.* **2010**, 132(48): 17216-17226.
- [13] Tang, Y.; Yang, H.; Shen, J.; Wu, B.; Ju, X.; Lu, C.; Cheng, G. 4-(1-Amino-5-Aminotetrazolyl) Methyleneimino-3-methylfuroxan and Its Derivatives: Synthesis, Characterization, and Energetic Properties. *Eur. J. Inorg. Chem.* **2014**, 2014(7): 1231-1238.
- [14] Fischer, D.; Klapötke, T. M.; Reymann, M.; Schmid, P. C.; Stierstorfer, J.; Sućeska, M. Synthesis of 5-(1H-Tetrazolyl)-1-hydroxy-tetrazole and Energetically Relevant Nitrogen-rich Ionic Derivatives. *Propellants Explos. Pyrotech.* **2014**, 39(4): 550-557.
- [15] Churakov, A. M.; Tartakovsky, V. A. Progress in 1,2,3,4-Tetrazine Chemistry. *Chem. Rev.* **2004**, 104(5): 2601-2616.
- [16] Fischer, N.; Fischer, D.; Klapötke, T. M. Pushing the Limits of Energetic Materials – the Synthesis and Characterization of Dihydroxylammonium 5,5'-Bitetrazole-1,1'-Diolate. *J. Mater. Chem.* **2012**, 22(38): 20418-20422.
- [17] Khakimov, D. V.; Pivina, T. S. Calculated Enthalpies of Formation of 5,5'-Bitetrazole Salts. *Mendeleev Commun.* **2016**, 26(2): 134-135.
- [18] Sinditskii, V. P.; Filatov, S. A.; Kolesov, V. I.; Kapranov, K. O.; Asachenko, A. F.; Nechaev, M. S.; Lunin, V. V.; Shishov, N. I. Combustion Behavior and Physico-chemical Properties of Dihydroxylammonium 5,5'-Bistetrazole-1,1'-diolate (TKX-50). *Thermochim. Acta* **2015**, 614: 85-92.
- [19] Shang, Y.; Jin, B.; Peng, R.; Guo, Z.; Liu, Q.; Zhao, J.; Zhang, Q. Nitrogen-rich Energetic Salts of 1H,1'H-5,5'-Bistetrazole-1,1'-diolate: Synthesis, Characterization, and Thermal Behaviors. *RSC Adv.* **2016**, 6(54): 48590-48598.
- [20] Shang, Y.; Jin, B.; Liu, Q.; Peng, R.; Guo, Z.; Zhang, Q. Synthesis, Thermal

- Behavior, and Energetic Properties of Diuronium 1H,1'H-5,5'-Bistetrazole-1,1'-diolate Salt. *J. Mol. Struct.* **2017**, *1133*: 519-525.
- [21] Fischer, D.; Klapötke, T. M.; Stierstorfer, J. Salts of Tetrazolone – Synthesis and Properties of Insensitive Energetic Materials. *Propellants Explos. Pyrotech.* **2012**, *37*(2): 156-166.
- [22] Gottfried, J. L.; Klapötke, T. M.; Witkowski, T. G. Estimated Detonation Velocities for TKX-50, MAD-X1, BDNAPM, BTNPM, TKX-55, and DAAF Using the Laser-induced Air Shock from Energetic Materials Technique. *Propellants Explos. Pyrotech.* **2017**, *42*(4): 353-359.
- [23] Niu, H.; Chen, S.; Jin, S.; Li, L.; Jing, B.; Jiang, Z.; Ji, J.; Shu, Q. Thermolysis, Nonisothermal Decomposition Kinetics, Calculated Detonation Velocity and Safety Assessment of Dihydroxylammonium 5,5'-Bistetrazole-1,1'-diolate. *J. Therm. Anal. Calorim.* **2016**, *126*(2): 473-480.
- [24] Gong, W.; Jin, B.; Peng, R. Deng, N.; Zheng, R.; Chu, S. Synthesis and Characterization of [60]Fullerene-poly(Glycidyl Nitrate) and Its Thermal Decomposition. *Ind. Eng. Chem. Res.* **2015**, *54*(10): 2613-2618.
- [25] Kissinger, H. E. Reaction Kinetics in Differential Thermal Analysis. *Anal. Chem.* **1957**, *29*(11): 1702-1706.
- [26] Doyle, C. D. Kinetic Analysis of Thermogravimetric Data. *J. Appl. Polym. Sci.* **1961**, *5*(15): 285-292.
- [27] Ozawa, T. A New Method of Analyzing Thermogravimetric Data. *Bull. Chem. Soc. Jpn.* **1965**, *38*(11): 1881-1886.
- [28] Jenkins, H. D. B.; Roobottom, H. K.; Passmore, J.; Glasser, L. Relationships Among Ionic Lattice Energies, Molecular (Formula Unit) Volumes, and Thermochemical Radii. *Inorg. Chem.* **1999**, *38*(16): 3609-3620.
- [29] Qiu, L.; Xiao, H; Gong, X.; Ju, X.; Zhu, W. Theoretical Studies on the Structures, Thermodynamic Properties, Detonation Properties, and Pyrolysis Mechanisms of Spiro Nitramines. *J. Phys. Chem. A* **2006**, *110*(10): 3797-3807.
- [30] Sinditskii, V. P.; Filatov, S. A.; Kolesov, V. I.; Kapranov, K. O.; Asachenko, A. F.; Nechaev, M. S.; Lunin, V. V.; Shishov, N. I. Dihydroxylammonium 5,5'-Bistetrazole-1,1'-diolate (TKX-50): Physicochemical Properties and Mechanism of Thermal Decomposition and Combustion. *Autumn Seminar on Propellants Explos. Pyrotech. 11th*, Qingdao, China **2015**, 221-233.
- [31] Wang, R.; Xu, H.; Guo, Y.; Sa, R.; Shreeve, J. M. Bis[3-(5-Nitroimino-1,2,4-Triazolate)]-based Energetic Salts: Synthesis and Promising Properties of a New Family of High-Density Insensitive Materials. *J. Am. Chem. Soc.* **2010**, *132*(34): 11904-11905.

Received: October 17, 2017

Revised: July 25, 2018

First published online: September 21, 2018